Materials and Structures (2025) 58:82
https://doi.org/10.1617/s11527-025-02605-0

ORIGINAL ARTICLE

Experimental characterization of VHPC reinforced with short synthetic fibers

V. Romanazzi · F. Micelli · S. Moro · P. Serna Ros · M. A. Aiello

Received: 4 June 2024 / Accepted: 11 February 2025 / Published online: 3 March 2025
© The Author(s) 2025

Abstract Very-High-Performance Concrete (VHPC) are defined as concrete capable of reaching compressive strength higher than 80 MPa. These performances can be reached thanks to its compact and extremely dense microstructure, as a result of a proper mix. Together with their great durability properties, these concretes may lead to reduce cross sections of structural elements and thus save material and built volumes. The addition of synthetic fibers allows to significantly increase the toughness and crack opening resistance, beyond the tensile strength. These benefits can easily be traduced in an improved durability of the VHPC concrete. the aim of this research activity is to enlarge the experimental database of high-performances concrete reinforced with synthetic fibers having different size. In fact, contrary to the case of steel fibers, few works are report ed in literature regarding the types of fibers investigated herein. In the present work three Very High-Performance Fiber Reinforced Concrete (VHPFRC) mixes have been studied and characterized in laboratory. The mixes were realized with the same VHPC concrete matrix and different types of synthetic fibers: 10 mm straight polyvinyl alcohol (PVA) fibers; 30 mm waved polypropylene (PP) fibers; 40 mm waved polypropylene (PP) fibers. The first mix was realized using PVA fibers only, the second with 30 mm PP fibers and the last one was obtained by mixing PVA fibers and 40 mm PP fibers. A further VHPC mix with no fibers has been also realized and tested as reference material. Compression tests on both cylindrical and cubic specimens and modulus of elasticity tests have been performed for each mix. The VHPFRC toughness have been determined by means of three-points bending tests according to EN 14651. The bending parameters obtained from the experimental test have been compared between all the mixes and an analysis of the fracture energy has been performed. Moreover, each mix has been tested at bending with four-points setup in order to verify the efficiency of this test type for VHPC reinforced with synthetic fiber. The results provided in the paper highlight the different effects, in terms of mechanical response, caused by fibers of different size at different cracking stages of the tested materials.

Keywords Very high-performance concrete · Synthetic fibers · Polypropylene and polyvinyl alcohol fibers · Bending behavior · Toughness

V. Romanazzi (✉) · F. Micelli · M. A. Aiello
Department of Innovation Engineering, University of Salento, Lecce, Italy
e-mail: vincenzo.romanazzi@unisalento.it

S. Moro
Master Builders Solutions, Treviso, Italy

P. Serna Ros
Instituto de Ciencia y Tecnología Del Hormigòn (ICITECH), Universitat Politecnica de Valencia, Valencia, Spain

1 Introduction

Very-High-Performance Fiber-Reinforced Concrete (VHPFRC) are defined as concrete capable of reaching compressive strength higher than 80 MPa with a discontinuous reinforcement of fibers (such as steel, basalt, glass, carbon, polypropylene, e.g.) immersed in the matrix. Their beneficial mechanical properties are mainly due to a compact and extremely dense microstructure that also provides to increase their resistance to aggressive liquid and gases penetration by reducing the presence of pores in concrete matrix [1]. Together with their great durability properties that reduce maintenance costs, the high compressive strength of these concrete allows to reduce cross sections of structural elements and thus save material [2].

As in case of plain concrete, crack width control plays a primary role in VHPC structures, since there is a close relationship between mean and maximum crack widths and the durability of the structure in terms of penetration of aggressive agents [3]. At this aim, fibers randomly distributed in concrete matrix showed to be effective in arresting cracks at both micro and macro-levels. At the microscopic scale, fibers prevent the initiation and growing of cracks, meanwhile at the macroscopic scale the "bridge effect" of the fibers allow to control the unstable cracks propagation and thus enhance concrete tensile strength, toughness and ductility [4–6]. The ability of fibers to withstand the cracks formation, opening and propagation in concrete depends on many factors, such as their material (modulus and tensile strength), aspect ratio, shape, content, and direction, etc. [7].

In construction industry, the two most used types of fibers are steel fibers and polymeric synthetic fibers. From the first research activities to the newest applications, steel fibers randomly distributed in the matrix lead to a significant impact on the mechanical properties of concrete when added in its mix design. In particular, it has been shown that steel fibers effectively controls cracks generation and development, improving the concrete tensile, flexural and impact strength and toughness [4, 8, 9]. Thanks to their mechanical properties, steel fibers have been diffusely used in civil and military concrete structures, including ports, cross-sea bridges and tunnels [10]. Steel fibers are generally protected from corrosion in presence of oxygen inside concrete by a compact thin film shield that guarantees the excellent performance of fiber-reinforced concrete. However, the presence of an aggressive chloride environment may cause the failure of this protection film and corrode the steel fibers, causing concrete durability degradation [11, 12]. At this purpose, several studies have been made regarding the durability of steel fibers reinforced concrete under aggressive environments. It has been observed that pitting or uniform corrosion of steel fibers led to a significantly decrease of the actual tensile strength of the fiber and, in case of pitting, to a brittle failure [13]. This clearly led to significant decrease in the mechanical strength of concrete reinforced with steel fibers [14, 15]. Moreover, steel are conductive in electric and magnetic field and thus their content in concrete had to be limited in structures such as tunnels and continuous slabs for high-speed railway systems, where the communication systems based on the transmission of electro magnetics waves can be disturbed [16].

In this context, synthetic fibers have been considered as reinforcement in VHPC to overcome these issues observed in steel fibers [17, 18]. Firstly, synthetic fibers have a lower density compared to steel fibers, resulting in a higher volume of fibers when used in concrete. In their work, Meng et al. [19] showed that high-performance synthetic fiber concrete has superior resistance to sulfate attack and freeze/thaw over the ordinary concrete due to excellent anti-crack performance and low permeability. Together with the durability properties, the research activities were conducted also on mechanical properties of synthetic fibers reinforced concrete, demonstrating that addition of synthetic fibers in concrete significantly enhance its tensile strength, flexural and shear strength and toughness [20–24]. Among the different polymeric fibers, polypropylene (PP) and polyvinyl alcohol (PVA), have attracted the attention of researchers and industry, because of their physical and mechanical advantages. In particular, the use of PP fibers in cement-based materials became widespread due to their resistance to a variety of chemical agents, sustainabe costs and easy processing. In fact, the PP fibers are characterized by an elastic modulus in the range of 1.5–12 GPa and a ultimate tensile strength between 240 and 900 MPa [25]. These fibers can be produced in several shapes, from straigth to crimped, embossed and textured with both circular and non-circular cross-sections [26]. As reported

in [22, 23], the crimped profile exhibited the highest energy absorption capacity in the pull-out tests. Behfarnia and Behravan [27] conducted a study investigating the impact of PP macro-fiber content on the compressive strength of concrete. Their findings revealed that there was no significant change in the compressive strength of concrete by varying fiber content when compared to control samples. Other authors [28, 29], observed that Incorporating PP macro-fibers into self-compacting concrete resulted in an improvement in compressngth, even if this result is not always meaningful.

Review of current studies indicated that synthetic fibers have a positive impact on chloride penetration and water permeability of concrete [30–34], which means that the service life of buildings can be extended.

This research introduces a novel investigation into the interaction of two different types of synthetic fibers within a very high-performance concrete (VHPC) matrix, an area that has seen limited exploration. Additionally, a novel aspect of this study is the comparison between two testing methodologies: the three-point bending test and the four-point bending test on unnotched specimens. This analysis provides new insights into the mechanical behaviour and performance of fiber-reinforced VHPC, contributing significantly to advancements in material engineering and testing protocols. To this aim, the mechanical properties of three different VHPFRC mixtures and a plain VHPC reference mix have been investigated. In particular, polypropylene (PP) and polyvinil-alchol (PVA) fibers has been used: one mix was realized with PP fibers only; the other with PVA fibers only and the last one with PP and PVA fibers combined. Compressive strength, modulus of elasticity, flexural strength and thougness have been measured and analyzed, including a comparison between the different proposed mixes. The flexural strength has been studied by performing both three-points bending and four-points bending tests. The results reported in this work show that all the mixes reached about 110 MPa of compressive strength. The mix with PP fibers only resulted to have a compressive strength and modulus of elasticity slightly lower than the other mixes. On the other hand, the flexural tests showed that short PVA fibers allow to better control the crack initial state, meanwhile the VHPFRC with long PP fiber was able to support high level of stress for higher value of crack opening. The mix realized with both types of fibers show an intermediate behavior, which confirmed the different role of the studied fibers during the service life of the material.

The authors developed also an analytical prediction on the mechanical properties of the proposed VHPFRC mixes, as well as an inverse finite element analysis. However, the main objective of this paper is to present and discuss the experimental work accurately in order to contribute for better understand some specific aspects related to FRC that still need further investigation. At present, a publication is under preparation on the impact behaviour of VHPFRC plates prepared with the mixes presented herein. A FEM analysis has been carried out to predict the state of damage as the fiber content and type change, from the experimental behavioural bonding of the materials.

2 Experimental programme

2.1 Materials and mix design

The geometrical and mechanical properties of the three types of fiber used in this experimental research are shown in Table 1. The fibers used in this work are

Table 1 Geometrical and mechanical properties of short fibers

Fiber name	Material	Length [mm]	Equivalent diameter [mm]	Aspect ratio	Shape	Tensile strength [MPa]	Elastic Modulus [MPa]
MF 401	Polyvinyl alcohol	12	0.20	60		800	27000
MF 236	Polypropylene	29	0.75	38.6		450	3250
MF 246	Polypropylene	40	0.75	53.3		450	3250

produced by Master Builder Solution®. The MasterFiber 401 are microfibers in polyvinyl alcohol (PVA) for concrete reinforcement with a length of 12 mm. These PVA microfibers are used to reduce crack formations in concrete due to shrinkage and increase its flexural strength. The Master Fiber 236 and 246 are macrofibers in polypropylene (PP) for concrete reinforcement with a length equal to 30 mm and 40 mm respectively. The waved shape improves the bond with the concrete matrix and so contrasts possible pull-out failures and enhances mechanical properties of concretes providing improved toughness and ductility.

Four VHPC mixtures have been studied, casted and tested; the mixes investigated had the same recipe shown in Table 2. Three mixtures have been added with fibers and the remaining one has been used as control mix.

As can be seen from Table 2, the mix VHPFRC_1 was composed by PVA microfibers only, VHPFRC_2 was realized adding 30 mm length PP macrofibers only and in the last mix, named VHPFRC_3, both PVA microfibers and 40 mm length PP macrofibers were used.

A higher dosage of the superplasticizer (i.e. 4% by weight of cement) was used in VHPFRC mixes aiming to achieve a flow of 60 cm or greater to guarantee the requirements of an SCC (Self-Compacting Concrete) also with the addition of fibers. A cylindrical compressive strength higher than 85 MPa is expected to be reached with this recipe (Fig. 1).

2.2 Specimens and test setup

A total of 67 VHPFRC specimens has been casted and tested within this experimental study. Each mix was tested under compression both with cubic (150 mm side) and cylindrical (150 mm diameter and 300 mm heigh) specimens. In particular, three cubes and five cylinders were tested for each mix. These tests were performed according to the standard UNI EN 12390–3 [35]. The test of modulus of elasticity, according to UNI EN 12390–13 [36], were performed on three cylindrical samples for each VHPC mixture before the compressive strength tests.

On the other hand, the flexural strength tests were done both with three-points bending test (3PBT) and four-points bending test (4PBT) setup. The 3PBT were performed on five notched beams for each

Table 2 VHPFRC mix design (quantities in kg/m^3)

Mix	CEM I 42.5N	Silica fume	Sand Aggregates			Superplasticizer	Water	Fibers (%V_f)		
			(< 0.5)	(0.6 < d < 1.2)	(1.2 < d < 4)			MF401	MF236	MF246
VHPC	800	175	305	365	225	25.0	170	–	–	–
VHPFRC_1	800	175	305	365	225	31.8	170	30 (2.3%)	–	–
VHPFRC_2	800	175	305	365	225	31.8	170	–	30 (3.0%)	–
VHPFRC_3	800	175	305	365	225	31.8	170	20 (1.5%)	–	10 (1.0%)

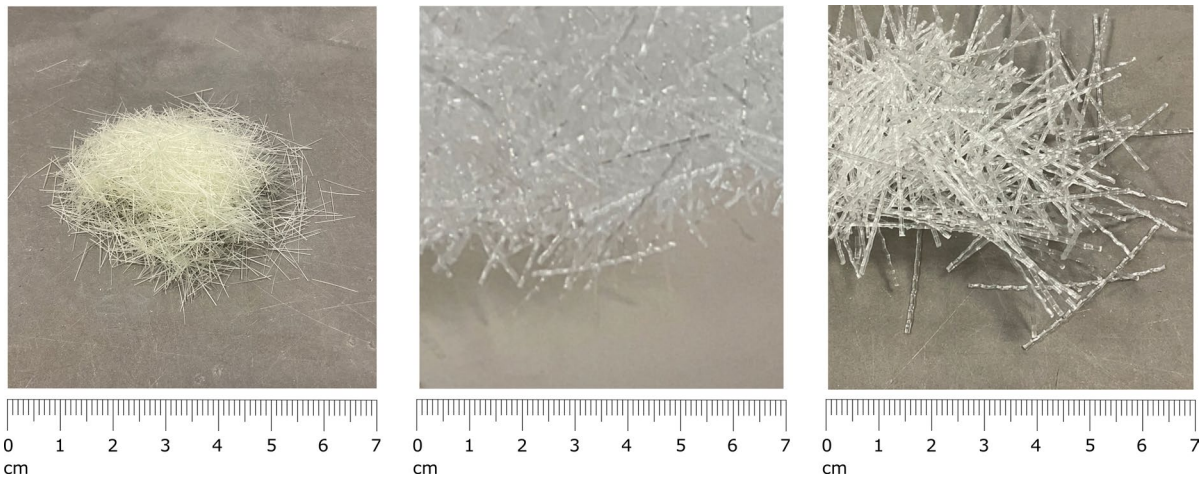


Fig. 1 **a** MasterFiber 401; **b** MasterFiber 236; MasterFiber 246

mixture using an INSTRON® 3389 hydraulic servo-controlled testing machine, in accordance with the UNI EN 14651 [37] standard. The tests were performed under crack mouth opening displacement (CMOD) control, with the following procedure:

An initial loading rate of 0.5 mm/min was applied until reaching 80% of the maximum load peak.
The loading rate was then reduced to 0.05 mm/min and maintained until the crack occurred.
Finally, the rate was increased to 0.2 mm/min and sustained until the total CMOD reached 4 mm.

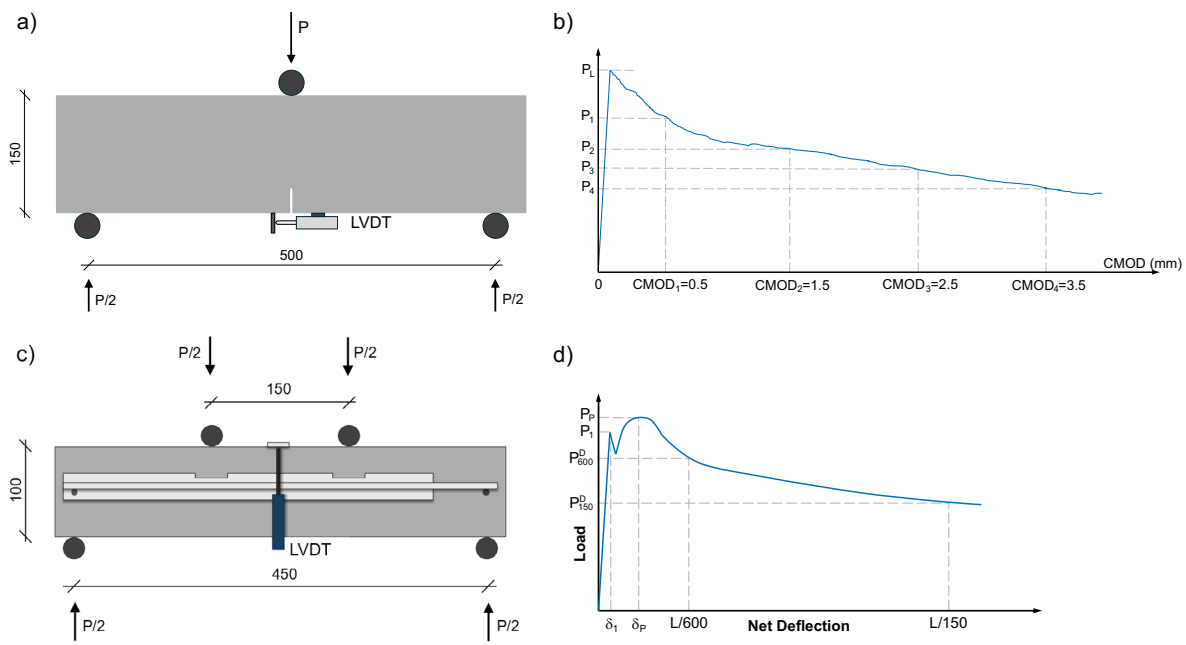


Fig. 2 **a** 3PBT test setup (measures in mm); **b** EN 14651 output graph for 3PBT on notched beams; **c** 4PBT setup (measures in mm); d) ASTM C1609 output graph for 4PBT

This stepwise approach ensured precise control of the crack propagation during the test. In particular, as can be seen from Fig. 2a, the CMOD has been measured by means of a linear variable displacement transducer (LVDT) positioned below the notch of the beam. From the measures w given by the LVDT it was possible to calculate the CMOD values with the formula:

$$CMOD = w \cdot (H/(H + i))$$

where H is the heigh of the beam (150 mm) and i is the distance between the bottom surface of the beam and the axis of the LVDT that has been measured for each specimen.

As suggested by the technical standard, the results of these tests are represented as flexural strength *vs.* CMOD graphs (Fig. 2b), where the flexural strength is determined as:

$$f_{fct,L} = \frac{3Pl}{2bh_{sp}^2}$$

in which P is the load measured by the loading machine, l is the span between the cylindrical supports (500 mm), b is the width of the cross Sect. (150 mm) and h_{sp} is the distance between the tip of the notch and the top of the specimen (125 mm).

The test setup used for 4PBT is shown in Fig. 2c. These tests were performed on five unnotched beams for each mix with a cross section of 100 mm x 100 mm and a span length of 450 mm. As reported in the ASTM C1609 [38], these tests were performed under displacement controls. In particular, the net deflection has been increased by 0.05 mm/min until the peak load was reached. After that, the rate of increase net deflection has been set to 0.2 mm/min up to the end of the test. Two LVDTs were positioned at the mid-span on the two sides of the specimen in order to measure the displacement δ. With the load P given by the universal testing machine it was possible to obtain the equivalent bending stress f:

$$f = \frac{PL}{bh^2}$$

where L is the span between the cylindrical supports (450 mm), b is the width of the cross section of the beam (100 mm) and h is specimen height. As shown in Fig. 2d, the results have been displayed by means of load-net deflection graphs and the parameters calculated according to the method shown in [38].

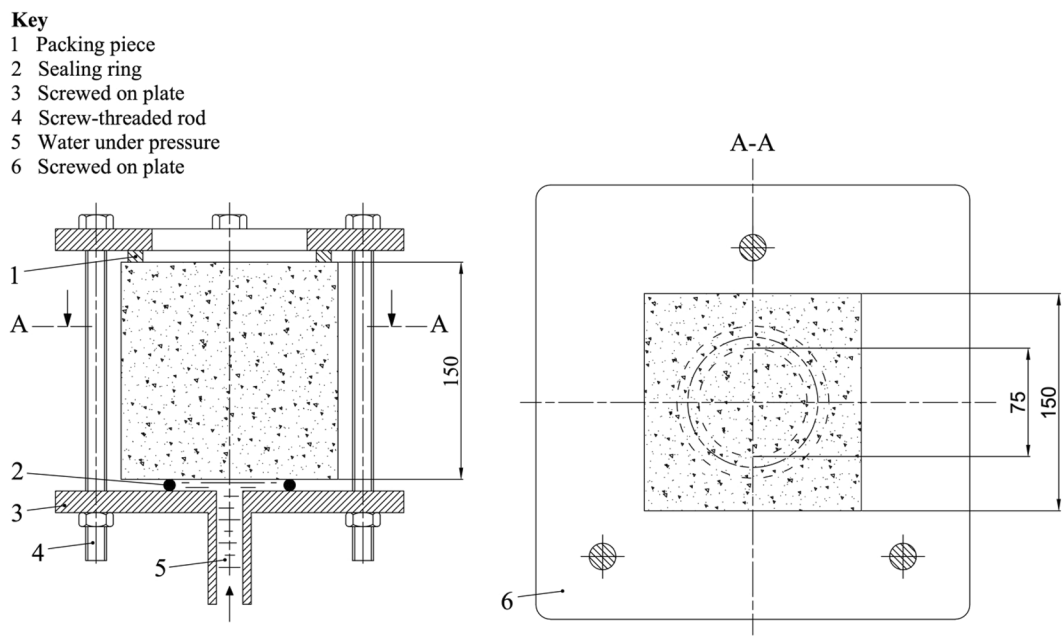


Fig. 3 Water permeability test setup according to UNI 12390–8 [39] (dimensions in mm)

Finally, the tests of permeability were run in order to check the durability of this new concretes; in this perspective, three cubic samples (150 mm sided) have been tested, for each VHPFRC mix, under water pressure conditions according to UNI EN 12390–8 [39]. The test setup defined in the standard is illustrated in Fig. 3. The cubic specimens were positioned in the testing device providing hermeticity at the borders to assure the water pressure application only at the bottom side. Controlled pressure water at 500 kPa was applied onto the specimen for 72 h continuously. Once the specimen has received the water pressure for the specified time, the specimen is retired from the testing device and the excess water is clean out. Thereafter, the specimen is split in half to measure the water penetration depth.

3 Experimental results

3.1 Slump flow test

The slump flow tests have been performed according to the EN 12350–8 [40]. In particular, the cone was filled with the concrete mix without tamping and removing any surplus from around the base of the cone. Once the cone has been filled, it was lifted and the final extension of the concrete spread circle was measured in two orthogonal directions. The average values obtained for each mix have been reported in Table 3.

As specified in the previous section, the comparison between the slump values obtained with VHPFRC mixes and plain VHPC mix has to be made considering the higher quantity of superplasticizer used in mixes with synthetic fibers. In particular, it can be seen that the largest reduction in workability has been observed in VHPFRC_1 and VHPFRC_3 mixes. Despite the increase in superplasticizer quantity, as referring to the plain VHPC mix results, the concrete spread circle diameter has been reduced of 26% and 34% in case of mix VHPFRC_1 and VHPFRC_3, respectively. On the other hand, the slump flow value obtained with VHPFRC_2 mix is almost the same as obtained with the mix without fibers.

The significative influence on the workability of the mix has also been observed by [41, 42]. They suggests that this difference could be the results of the extremely high surface area of PVA fibers and their capacity to absorb water in the early stage in respect to PP macrofibers.

3.2 Compressive strength and elastic modulus

The results of the mechanical characterization of the VHPC mixes introduced in the previous section are reported in Table 3. As defined in the previous section, both the cubic compressive strength (R_c) values and modulus of elasticity (E_c) are obtained as average of three specimens, meanwhile the cylindrical strength (f_c) results are average values of five specimens. Moreover, in Table 3 there is also reported the ratio between the cylindrical and cubic compressive strength f_c/R_c obtained for each concrete mix.

From the compressive strength results shown in Table 3, it can be seen that all the VHPC mixes were able to reach the 85 MPa target, referring to the cylindrical compressive strength. In particular, it results that the average cubic compressive strength of VHPFRC_1 with PVA microfiber was 1% lower than the reference mix VHPC. On the other hand, larger decay

Table 3 Average results of slump flow test and mechanical characterization (CoV values in parentheses)

	Slump flow [mm]	Compressive strength [MPa]			Elastic Modulus E_c [GPa]
		R_c [MPa]	f_c [MPa]	f_c / R_c [–]	
VHPC	840	121.4 (4.1%)	110.8 (4.3%)	0.91	44.23 (0.9%)
VHPFRC_1	620	119.9 (6.0%)	106.9 (4.9%)	0.89	41.45 (1.7%)
VHPFRC_2	820	108.4 (1.2%)	91.1 (17.2%)	0.84	40.41 (2.1%)
VHPFRC_3	550	111.0 (2.7%)	94.3 (16.1%)	0.85	42.31 (2.0%)

of about 11% and 9% has been observed in case of VHPFRC_2 and VHPFRC_3 respectively. These differences can be considered as logical variability among the four castings, also considering the coefficient of variation calculated for each concrete mix and reported in Table 3. In their work, [6] and [43] observed a slightly decrease of compressive strength due to the presence of macro-synthetic fibers. In particular, they reported that fibers constitute an inclusion that may act as a structural discontinuity, which produces a lower strength under compression forces. According to [40] and [41], the low modulus of elasticity of the reinforcing fibers and the introduction of small number of voids into the concrete around the fibers is probably responsible for the observed strength reduction. At the same time, in [44] observed that the macro-plastic fibers have no obvious effects on the compressive strength.

As can be seen from the elastic modulus results shown in Table 3 the same trend already observed for compressive strength results have been obtained. In fact, despite the low scatter between the four concrete mixes, also in this case the results obtained for VHPFRC_2 mix is slightly lower than the other two fiber reinforced mixtures. This observation confirms what has already been discussed previously regarding the effect of macro-polypropylene fibers in concrete. Finally, as compared with the reference plain VHPC mixture, the results obtained with mixes VHPFRC_1, VHPFRC_2 and VHPFRC_3 are 6%, 9% and 4% lower, respectively. In terms of design consideration, it is clear that these differences appear meaningless, if addressed to practitioners interested in practical applications.

3.3 Three-points bending tests on notched beams

As previously reported, three-points bending tests on notched beams were performed on five samples for each VHPFRC mix. Overall, as can be noted in Fig. 4, all the curves are characterized by a large load decay and a corresponding increase in CMOD values. However, this loss of control always ends before

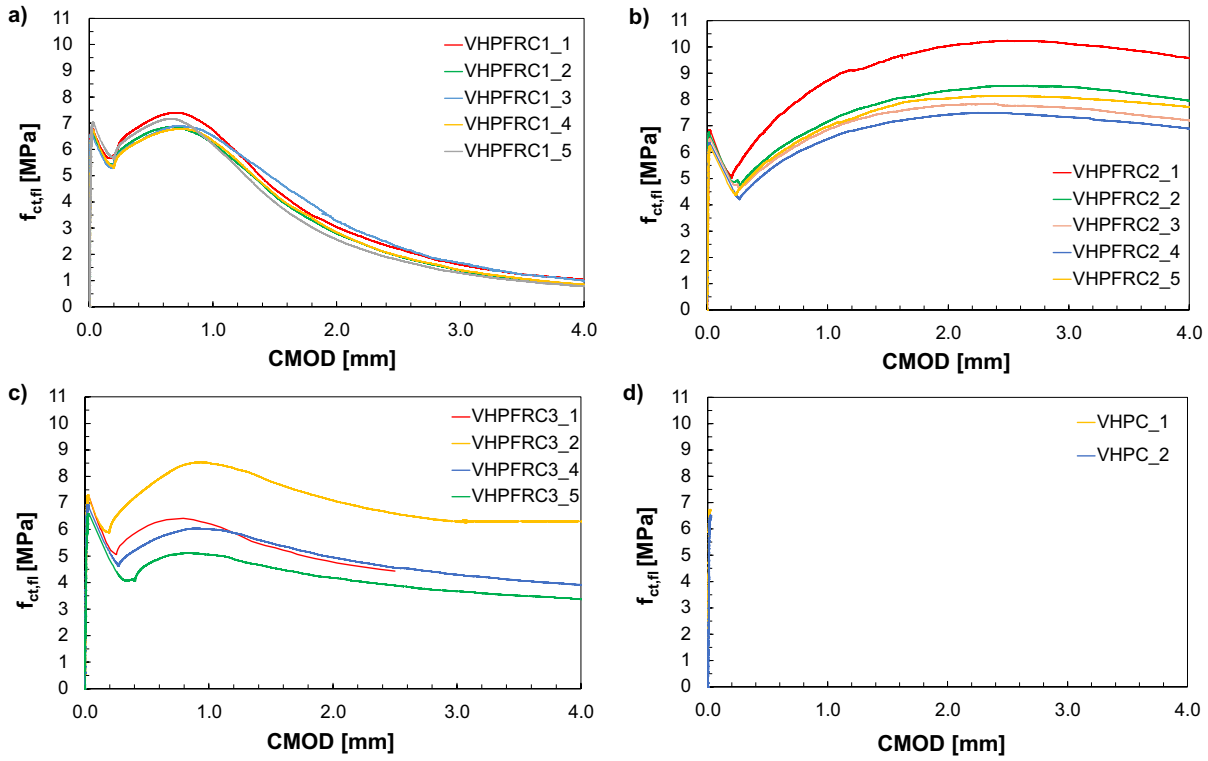


Fig. 4 3PBT results for: **a** VHPFRC_1; **b** VHPFRC_2; **c** VHPFRC_3; **d** VHPC

cracks reach 0.5 mm opening and the analysis of the results (i.e. especially referring to f_{R1} values) are considered valid. Another aspect to be considered is that, given the high difference between concrete and fibers elastic moduli, the load transfer between concrete matrix that reaches its tensile strength and the fibers appears to be retarded. This aspect is also confirmed by other authors in literature [24, 45], and seems to be an intrinsic characteristic of synthetic fibers reinforced concrete.

The results obtained with the VHPFRC_1 mixture with the short PVA fibers are reported in Fig. 4a and in Table 4 in terms of flexural stress corresponding to the limit of proportionality (LOP) and the values of $CMOD_1$, $CMOD_2$, $CMOD_3$ and $CMOD_4$. As can be seen from the graph, the dispersion of the results for this group of specimens was very low, contrary to what is expected in this type of tests. A sharp stress decay has been observed after the LOP from about 7 MPa to 5.5 MPa in all specimens. As previously explained, this is probably due to the large difference between the VHPC matrix elastic modulus and the PVA fibers modulus. Once the first crack occurred in concrete matrix, in fact, in correspondence of the crack the load is carried only by the PVA microfibers, but the lower elastic modulus delayed their response. The contribution of the MasterFiber 401 is prevalent for low values of CMOD, between 0.2 mm and 1.2 mm, because of the length of the fibers. For higher value of crack opening, in fact, the microfibers contribution decrease and resulted to be significantly lower than in case of PP fibers.

The results obtained with the specimens prepared with VHPFRC_2 are shown in graph of Fig. 4b and in Table 4. As previously observed for VHPFRC_1 mix, also in this case a low dispersion of the results is obtained. The stress decay that occurred after the first crack formation in the concrete matrix is sharper than in case of VHPFRC_1 as the flexural stress decrease from about 7 MPa to 4.5 MPa. In this case, both the greater length and the waved profile of the fibers significantly contributed to increase the tensile flexural stress also for high CMOD values. In fact, despite the lower mechanical properties of the MF 236 fibers respect to the MF401 (Table 1), the higher bond with the VHPC matrix allowed to transfer higher stresses within the crack. The result confirmed what observed in [22], where the interface toughness and pullout load of structural macro-synthetic fibers were highly improved when they had a crimped profile.

On the other hand, Fig. 4c shows the results obtained on mix VHPFRC_3 realized with both PVA microfibers MF401 and PP macrofibers MF246. Unfortunately, the experimental data of specimen VHPFRC_3_3 have gone lost after the test, meanwhile the test of specimen VHPFRC_3_1 stopped after reaching CMOD value of 2.5 mm for an error occurred on the software of the testing machine. As can be seen from the graph and from the experimental values reported in Table 4, this mix exhibited an overall behavior that is included between a lower and upper limit defined by the results of VHPFRC_1 and VHPFRC_2 specimens group, respectively. In fact, after the LOP and the load decay already observed in the other mixes, the PVA microfibers allowed to quickly recover the load. In the second phase of the test, when the crack mouth opening is larger than 1 mm the stresses decreased as happened with VHPFRC_1 mix (Fig. 4a) since the MF401 fibers were no longer able to carry the load for the reasons previously discussed. At this point, the load decreasing seemed to reach an asymptote thanks to the contribution of the PP macrofibers.

Table 4 Average results of 3PBT on notched beams (CoV values in parentheses)

MIX	LOP [MPa]	f_{R1} [MPa]	f_{R1k} [MPa]	f_{R2} [MPa]	f_{R3} [MPa]	f_{R3k} [MPa]	f_{R4} [MPa]	f_{R3k} / f_{R1k} [–]
VHPC	6.71 (2.8%)	–	–	–	–	–	–	–
VHPFRC_1	6.77 (2.4%)	6.77 (3.8%)	6.30	4.38 (7.5%)	2.03 (10.2%)	1.66	1.11 (10.9%)	0.3
VHPFRC_2	6.54 (4.0%)	5.83 (11.0%)	4.68	7.97 (11.5%)	8.43 (12.8%)	6.50	8.13 (13.2%)	1.4
VHPFRC_3	7.04 (4.8%)	5.97 (20.8%)	3.73	5.82 (24.0%)	4.87 (24.4%)	2.73	4.63 (31.6%)	0.7

Finally, in Fig. 4d there are shown the results obtained with the reference VHPC mix without fibers. For the specimen VHPC_3 CMOD data recorded are not available due to an error in the readings of the clip gauge, for this reason this specimen is not included in the graph. Anyway, it is clear that the absence of fibers resulted in a totally brittle behavior without any post-cracking stage, as expected form theory.

In Fig. 5 representative specimens for each mix are shown after failure. In particular, Fig. 5a shows a specimen with only PVA microfibers that are barely visible due to their small section and length. Almost all the MF401 fibers that across the final crack resulted to be integer, meaning that the fibers were pulled-out from the concrete as previously discussed. Again, this observation confirms that the lower bond between PVA fibers and the concrete matrix prevented from fully exploiting their high mechanical properties. On the other hand, the PP macrofibers are clearly visible from Fig. 5b. In this case it can be noted that there are many fibers that were pulled-out from the concrete matrix and the remaining part that reached the tensile failure. This confirms the good bond developed between the waved MF236 and the VHPC. Finally, in Fig. 5c the VHPFRC_3 specimen, containing a mix of PVA and PP fibers, after failure is shown. The observation of the cracked surface of this specimen confirmed what has already been seen in the other pictures: the PVA microfibers are all pulled-out, meanwhile the MF246 are partially integer (slippage from concrete) and partially failed in tension.

Together with the mean values obtained from the tests, in Table 4 there are reported the characteristic values f_{R1k} and f_{R3k} calculated according to Eurocode 0 [46] and their ratio used by Model Code 2010 [47] for fiber reinforced concrete characterization. In particular, according to the Model Code, fiber reinforcement can substitute (also partially) conventional reinforcement at ultimate limit state, if f_{R3k} / f_{R1k} is higher than 0.5. Given the results shown in Table 4, this applies only to VHPFRC_2 and VHPFRC_3 mix design.

3.4 Four-points bending tests on unnotched beams

The results obtained with the four-points bending tests on unnotched specimens are shown in Table 5 and in graphs of Fig. 6. In particular, the numerical results are expressed in Table 5 in terms of peak load P_P, net deflection at peak load δ_P, peak strength f_P,

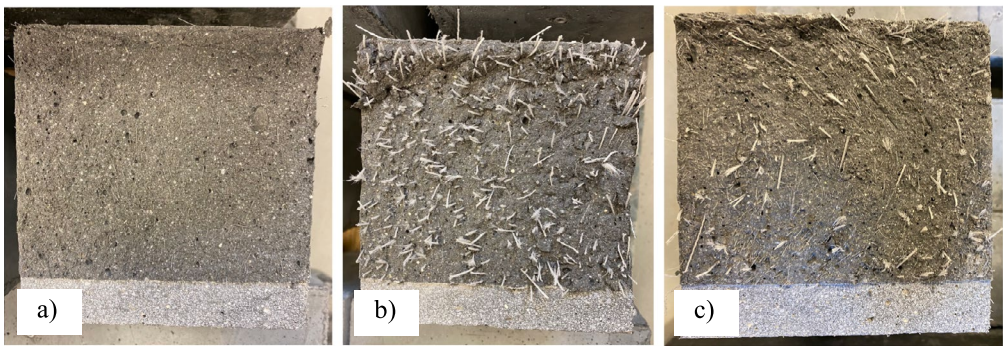


Fig. 5 Notched beam specimens after 3PBT failure: **a** VHPFRC_1; **b** VHPFRC_2; **c** VHPFRC_3

Table 5 Average results of 4PBT on notched beams (CoV values in parentheses) – ASTM C1609 [38]

MIX	P_P [kN]	δ_P [mm]	f_P [MPa]	P_{600} [kN]	f_{600} [MPa]	P_{150} [kN]	f_{150} [MPa]	T_{150} [J]
VHPFRC_1	26.7 (5%)	0.11 (31%)	12.0 (5%)	15.1 (25%)	6.8 (25%)	2.7 (29%)	1.2 (29%)	31.2 (18%)
VHPFRC_2	23.5 (9%)	0.08 (16%)	11.0 (6%)	18.6 (11%)	8.4 (11%)	21.7 (15%)	9.8 (15%)	61.2 (10%)
VHPFRC_3	22.2 (9%)	0.08 (21%)	10.1 (9%)	18.8 (21%)	8.5 (21%)	8.8 (21%)	6.2 (21%)	49.9 (21%)

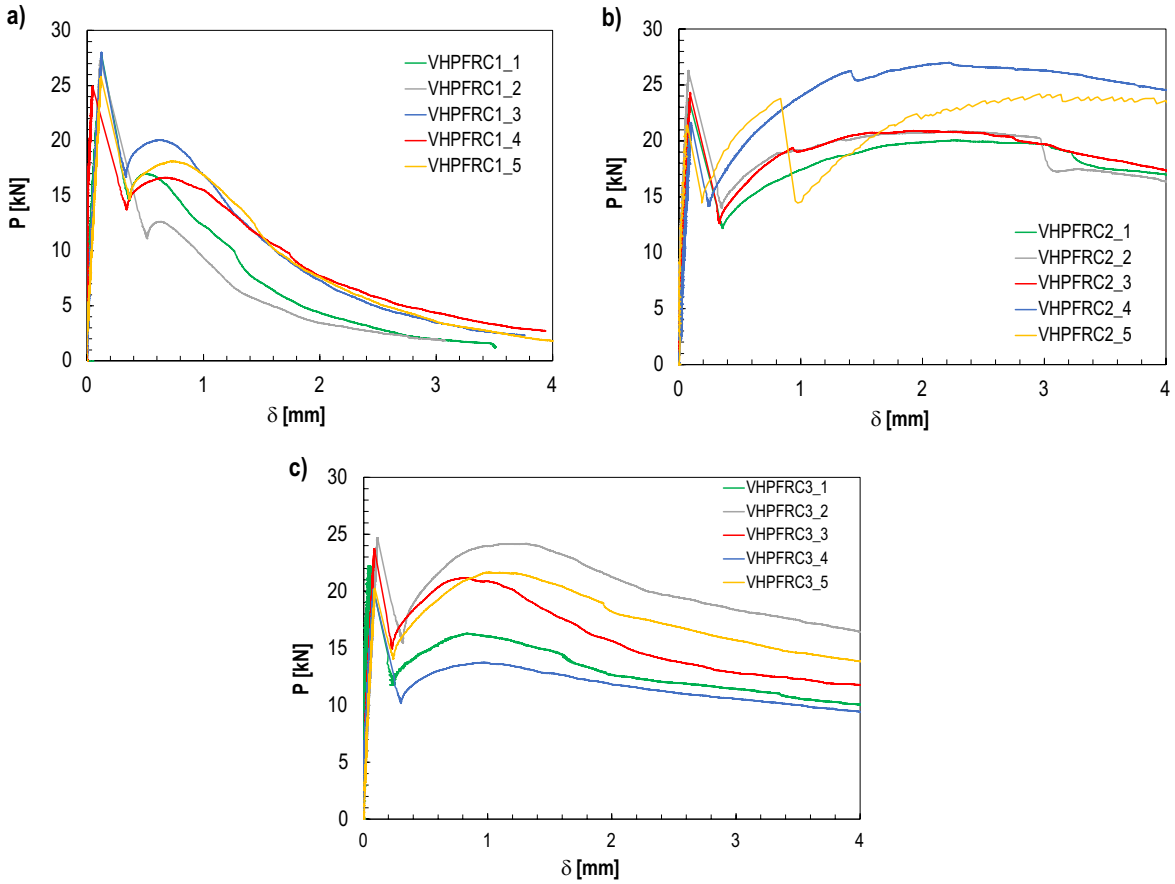


Fig. 6 4PBT results for: **a** VHPFRC_1; **b** VHPFRC_2; **c** VHPFRC_3

residual load P_{600} and strength f_{600} at the net deflection L/600, residual load P_{150} and strength f_{150} at the net deflection L/150 and toughness T_{150} calculated as the area under the load–deflection curve up to the net deflection of L/150. All the tests were considered valid since in all the specimens the cracks appeared in the constant moment zone. Moreover, from the curves reported in Fig. 6 it can be seen that, except specimen VHPFRC2_4, in all the tests the first peak load P_1 resulted to be equal to the peak load P_P (Fig. 2d).

The results obtained with VHPFRC_1 are shown in Fig. 6a other than in Table 5. The flexural behaviour observed in the mix realized with only PVA microfibers is characterized by different stages. After the first elastic stage, the first crack occurred and the stress sharply decrease as also observed in three-points bending tests. This deep decay in flexural stress is partially recovered in the following post-cracking stages. In fact, the stress increased until the deflection recorded reached about 1 mm and then decrease again up to the failure. This behaviour appeared to be significantly brittle as compared with the results obtained with the other two VHPFRC mixes.

In fact, as can be seen from Fig. 6b, the VHPFRC_2 specimens realized with only PP macrofibers were able to totally recover the maximum flexural stress after the first crack occurred. This can be observed also from Table 5 in which P_{600} and P_{150} values are almost equal to P_P. Moreover, the VHPFRC_2 mix specimens were able to carry the load for higher deflection showing a global more ductile behaviour.

Finally, as in case of three-points bending tests, the results obtained with VHPFRC_3 seemed to be the average of the previously discussed mixes. In fact, in the flexural stress *vs.* displacement curves of Fig. 6c there are evident both the contributes of PVA microfibers and PP macrofibers.

The differences between the three mixes are also confirmed by the toughness values T_{150} reported in Table 5. In particular, the area under the load-net deflection curves in case of VHPFRC_2 mix resulted to be twice the respective values obtained in case of VHPFRC_1 mix. Finally, the T_{150} value of VHPFRC_3 specimens resulted to be almost the average value between the other two VHPFRC mixes.

3.5 Water permeability tests

Water permeability tests were run in order to reveal the effects of the low porosity of such concrete targeted, which are targeted to be considered "zero maintenance". After the application of water under pressure for 72 h the specimens were splitted into and no water penetration depth was detected under the wet surface. This means that it was not possible to define a water penetration depth profile for the four mixes, both with and without synthetic fibers since the water permeability can be considered negligible. This can be easily explained since the composition of the VHPC mix design was characterized by a very low percentage of void and didn't allow the water to penetrate inside the specimens although applied in pressure continuously for a long period.

These results confirmed what already observed by other authors. In particular, in their work Sun and Xu [30] reported that PP fibers significantly alter the microstructure of concrete by reducing the amount, size and orientation of CH crystals and micro voids. This can be traduced in a global reduction of the voids and micro-cracking at the interfacial transition zone between the aggregates and the cement paste.

4 Analysis and discussion of test results

4.1 Bending tests results comparisons

In order to compare the results obtained on bending tests on the three VHPFRC mixes, the average curves of the experimental results of each mix obtained from both the bending test configurations are illustrated in Fig. 7. The differences already discussed become clearer by observing these graphs. In fact, it can be seen that the first linear elastic stage is the same for the three mixes in terms of both the LOP and the slope of the initial branch.

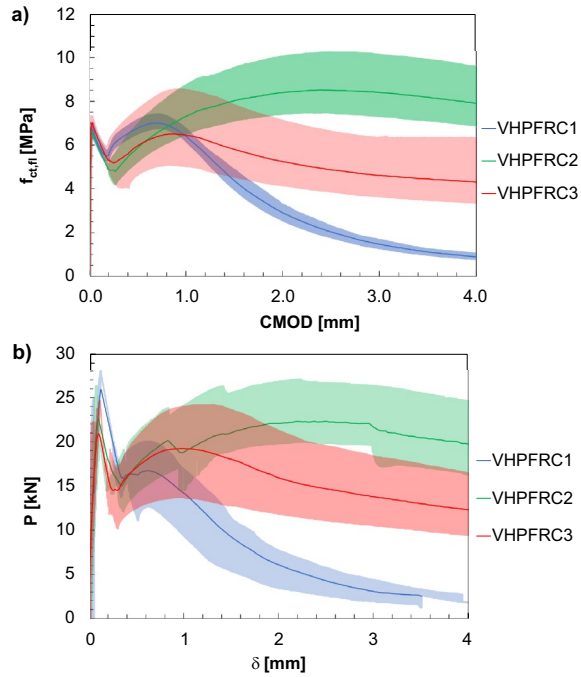


Fig. 7 Average curves of bending results on VHPFRC mix from: **a** 3PBT according to EN 14651; **b** 4PBT according to ASTM C1609

Once the crack occurred, it can be seen how the PVA microfibers allowed to better control the load decay and to recover the load quicker than the other mixes. Finally, the evident differences in the post-cracking behaviour for high value of crack opening width can be seen. The PP macrofibers included in mix VHPFRC_2 allowed the specimens to carry higher load from CMOD equal to 1 mm to the end of the tests. On the other hand, the mix VHPFRC_3, prepared with both PVA microfibers and PP macrofibers, seemed to stay in the middle between the other two VHPFRC mixes. Despite the contribution of the PVA microfibers appeared not so evident in this mix since no significant differences are seen for low CMOD values, the influence of MF246 can be noted for larger CMOD when the curve is compared with that one of VHPFRC_1.

As noted in the previous section regarding the results of three-points bending tests on VHPFRC mixes, in all the tensile flexural stress vs. CMOD experimental curves a deep stress decay has been observed after reaching the LOP. As also observed in [22], this phenomenon is probably linked to the

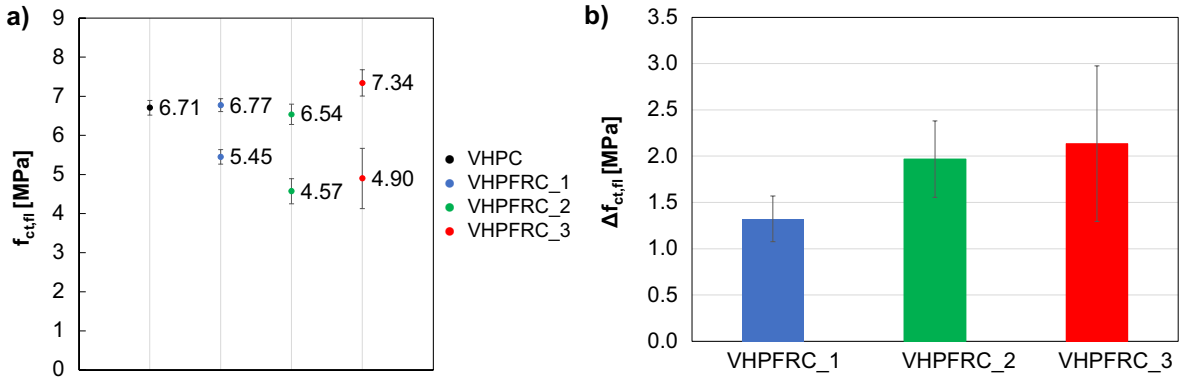


Fig. 8 Analysis of stress decay after LOP of VHPFRC mixes: **a** LOP value and respective lower point after decay; **b** stress decay quantified for each mix

difference between the VHPC matrix elastic modulus and the synthetic fibers and to the non-optimal adhesion forces between fibers and concrete matrix. At this purpose, in Fig. 8 there are reported two graphs aiming to analyze the load decay observed for the several mixes during the three points bending tests. In particular, in Fig. 8a two points of each average curve are reported corresponding to the LOP value and the lowest point after the stress decrease, meanwhile in Fig. 8b the difference between those two values is reported.

As regards the MF 401, in the previous section it has been just reported that the VHPC matrix modulus resulted to be higher than 40 GPa meanwhile the elastic modulus of PVA is equal to 27 GPa, that is about 33% lower. This means that once the first crack occurred in concrete matrix the load should be instantly carried by the PVA microfibers, but the lower elastic modulus delayed their response and this causes the load drop.

In the case of PP macrofibers this difference is even higher than the case of PVA microfibers. In fact, as shown in Table 1, the nominal elastic modulus of fibers MF236 is equal to 3.25 GPa that is more than one order of magnitude lower than the VHPC matrix elastic modulus. These observations explain why the stress decay is slightly reduced in case of VHPFRC_1 mix, as can be seen from Fig. 8. In fact, this mix has been prepared with PVA microfibers only and their higher modulus of elasticity allow to better control the load losses after the formation of the first crack.

Overall, considering the statistical variability reported in graph of Fig. 8b, this difference seems to be minimal despite the large scatter between the elastic moduli. This can be explained by the fact that, together with the fiber elastic modulus influence just discussed, the load recovery after the peak strictly depends also on the fibers volume and their bond with concrete matrix. In this case, VHPFRC_1 mix fiber volume is lower than in case of VHPFRC_2 and VHPFRC_3 (Table 2) and the crimped profile of PP is known to offer an higher bond capacity between the concrete matrix and the fiber.

4.2 Fracture energy

In order to analyze the post-cracking behavior of the three-points bending tests experimental results, the fracture energy has been calculated for each specimen according to the procedure defined in the Rilem Recommendation TC-50 [48]. In this recommendation the fracture energy is defined as the amount of energy necessary to create one unit area of a crack, meanwhile the area of a crack is defined as the projected area on a plane parallel to the main crack direction. In order to calculate the fracture energy the curves of the three-points bending tests shown in Fig. 4 have been converted into load F vs. deflection δ curves by means of the conversion criteria from CMOD to δ reported in [37]. The fracture energy $G_{F,j}$ has been calculated for different δ_j corresponding to the $CMOD_j$ (j = 1, 2, 3, 4). In particular, as suggested by the Rilem Recommendation the following equation was used:

$$G_{F,j} = \left(W_{0,j} + mg\delta_j\right)/A_{\text{lig}}$$

where $W_{0,j}$ is the area obtained from load vs. δ curves up to the corresponding δ_j value; m is the weight of the specimen; g is the gravity acceleration; δ_j are the deflection valued corresponding to $CMOD_j$ (j = 1, 2, 3, 4) previously defined; A_{lig} is the area of the ligament (i.e. specimen cross section minus the area of the notch).

The results obtained are shown in the histogram of Fig. 9. The results of the fracture energy allowed to have a measurement of the toughness of the VHPFRC mixes investigated. As can be clearly seen from Fig. 9, the fracture energy results confirmed what already observed from the comparison made regarding the average curves reported in Fig. 7. In particular, the fracture energy resulted almost the same for CMOD equal to 0.5 mm since in the first stage of the test is mainly governed by the VHPC matrix. The values determined for VHPFRC_1 mix were slightly higher than the others since the contribution of the PVA microfibers is relevant in this first stage of crack formation. This trend is inverted for the fracture energy values determined at crack mouth opening equal to 2.5 mm. In fact, despite the little differences, the VHPFRC_2 fracture energy values overcome those obtained on VHPFRC_1 and VHPFRC_3. This is due to the fact that in this stage the PP macrofibers contribution started to significantly increase meanwhile the PVA microfibers effects decreased. The same trend continued until the end of the tests since the fracture energy of VHPFRC_2 mix increased until it became almost the double of that one measured for VHPFRC_1 mix. On the other hand, the fracture energy of VHPFRC_3 mix specimens realized with 20 kg/m^3 of PVA microfibers and 10 kg/m^3 of PP macrofibers followed about the same trend of VHPFRC_1 except for the slightly higher increase for CMOD values 2.5 mm and 3.5 mm thanks to the contribution of MF246 fibers.

5 Conclusions

An extended experimental campaign has been conducted to investigate the mechanical properties of very high-performance fiber reinforced concrete (VHPFRC) incorporating different types and combination of synthetic fibers. The study involved three types of synthetic fibers: two types of waved polypropylene macro-fibers with crimped profiles and lengths of 30 mm and 40 mm, respectively, and straight polyvinyl alcohol microfibers with a length of 12 mm. The same VHPC concrete mixture was used as concrete matrix and three different mixes were defined: one with only PVA microfibers (L = 12 mm), one with only PP macrofibers (L = 30 mm), and one with a combination of both fiber types (PP L = 40 mm). The characterization at the hardened state included tests for compressive strength, modulus of elasticity, water permeability, tensile flexural strength, and toughness through three-point and four-point bending tests. The role of synthetic fibers was investigated by analyzing the post-peak behavior of the bending tests,

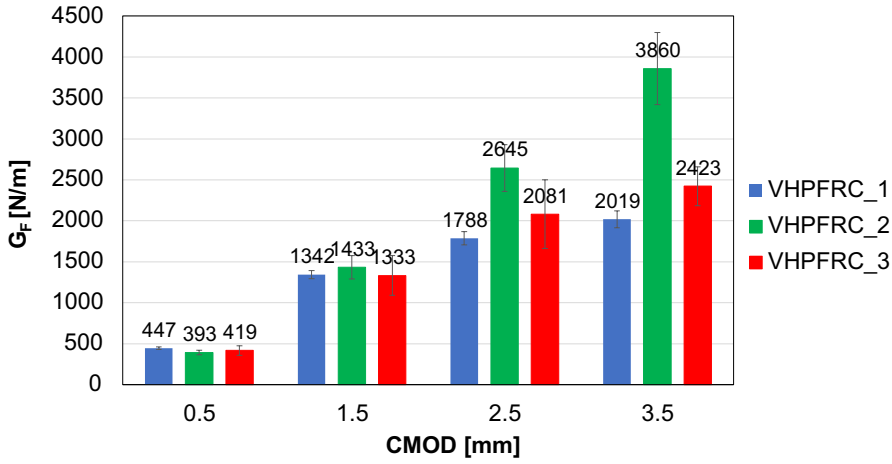


Fig. 9 Fracture energy analysis of three-points bending tests according to [48]

specifically by calculating the fracture energy according to RILEM guidelines.

Based on the experimental results herein shown and discussed, the following conclusions can be drawn:

- The presence of the short fibers in all cases brought beneficial effects since the toughness and fracture energy of VHPFRC were always higher when compared to VHPC matrix.
- All VHPC mixes achieved the target compression strength of 100 MPa. Notably, the average cubic compressive strength of VHPFRC_1, which included PVA microfibers, was slightly lower by 1% compared to the reference mix VHPC. In contrast, larger reductions of approximately 11% and 9% were observed in the case of VHPFRC_2 and VHPFRC_3, respectively. This minimal impact of the macro-propylene fibers on compressive strength aligns with findings from previous studies.
- As regards the three-points bending tests, it has been observed that once the crack occurred, the PVA microfibers allowed to better control the nearly post-peak behavior. At this stage an immediate load decay occurs, and PVA fibers were able to recover the load quicker than the other mixes. Additionally, notable distinctions in post-cracking behavior were observed, particularly for higher values of crack opening displacement. The mix incorporating PP macrofibers exhibited the ability to carry higher load from CMOD equal to 1 mm to the end of the tests. Finally, the mix realized with both PVA and PP fibers resulted in an intermediate mechanical response between the other two mixes.
- The results of the four points bending tests confirmed the same trend observed in three-points bending tests. In particular, the residual load at L/150 net deflection resulted to be very low in case of VHPFRC_1 mix and comparable to the first peak load of VHPFRC_2. The mix VHPFRC_3prepared with both macro and micro synthetic fiber types confirmed to have a post-peak behavior which falls in between respect to VHPFRC_1 and VHPFRC_2.

The results of the study revealed a different role in terms of toughness and crack control of synthetic fibers that can be incorporated into a concrete matrix. The nature of the fibers, their dimensions and their shapes can be considered important variables in order to design a proper mix, that can be optimized respect to the expected service conditions.

The tested VHPFRC materials demonstrated also to be non-permeable to water, which is an important requirement for the purpose of extending the life-cycle of buildings and reduce their maintenance. For this reason the proposed mixes can be considered for both pre-cast or on-site applications, assuring high sustainability due to high durability, and enhanced toughness and cracking control. In this perspective these materials are inspired to a class of "zero maintenance" concrete which should be considered mandatory in future design applications.

Future research in the field would include new fibers dosages, testing on real scale reinforced slab for each mix under punching shear load, in order to evaluate the fibers contribution also on concrete shear strength. Moreover, the authors are running FEM analysis to calibrate an accurate prediction of the experimental results, starting from an inverse analysis.

Funding Open access funding provided by Università del Salento within the CRUI-CARE Agreement.

Open Access This article is licensed under a Creative Commons Attribution 4.0 International License, which permits use, sharing, adaptation, distribution and reproduction in any medium or format, as long as you give appropriate credit to the original author(s) and the source, provide a link to the Creative Commons licence, and indicate if changes were made. The images or other third party material in this article are included in the article's Creative Commons licence, unless indicated otherwise in a credit line to the material. If material is not included in the article's Creative Commons licence and your intended use is not permitted by statutory regulation or exceeds the permitted use, you will need to obtain permission directly from the copyright holder. To view a copy of this licence, visit http://creativecommons.org/licenses/by/4.0/.

References

1. Yoo D-Y, Shin W, Chun B (2020) Corrosion effect on tensile behavior of ultra-high-performance concrete reinforced with straight steel fibers. Cem Concr Compos 109:103566. https://doi.org/10.1016/j.cemconcomp.2020.103566

2. Yoo DY, Banthia N (2016) Mechanical properties of ultra-high-performance fiber-reinforced concrete: a review. Cem Concr Compos 73:267–280. https://doi.org/10.1016/j.cemconcomp.2016.08.001
3. Li VC, Stang H, Krenchel H (1993) Micromechanics of crack bridging in fibre-reinforced concrete. Mater Struct 26(8):486–494. https://doi.org/10.1007/BF02472808
4. Uygunoğlu T (2008) Investigation of microstructure and flexural behavior of steel-fiber reinforced concrete. Mater Struct/Mater Constr 41(8):1441–1449. https://doi.org/10.1617/s11527-007-9341-y
5. Çelik Z, Bingöl AF (2020) Fracture properties and impact resistance of self-compacting fiber reinforced concrete (SCFRC)". Mater Struct/Mater Const 53(3):14878. https://doi.org/10.1617/s11527-020-01487-8
6. Banthia N, Gupta R (2004) Hybrid fiber reinforced concrete (HyFRC): Fiber synergy in high strength matrices. Mater Struct Mater Const 37(274):707–716. https://doi.org/10.1617/14095
7. Yoo DY, Banthia N (2019) Impact resistance of fiber-reinforced concrete – a review. Cem Concr Compos 104:103389. https://doi.org/10.1016/j.cemconcomp.2019.103389
8. Buratti N, Ferracuti B, Savoia M (2013) Concrete crack reduction in tunnel linings by steel fibre-reinforced concretes. Constr Build Mater 44:249–259. https://doi.org/10.1016/j.conbuildmat.2013.02.063
9. Zhang S, Zhang C, Liao L (2019) Investigation on the relationship between the steel fibre distribution and the post-cracking behaviour of SFRC. Constr Build Mater 200:539–550. https://doi.org/10.1016/j.conbuildmat.2018.12.081
10. Marcos-Meson V, Solgaard A, Fischer G, Edvardsen C, Michel A (2020) Pull-out behaviour of hooked-end steel fibres in cracked concrete exposed to wet-dry cycles of chlorides and carbon dioxide – mechanical performance. Constr Build Mater 240:117764. https://doi.org/10.1016/j.conbuildmat.2019.117764
11. Yang L, Zhang Z, Gao D, Tang J, Chang H, Liu G (2022) Mechanical property evolution and chloride transport of steel fiber-reinforced concrete exposed to simulated marine environments. Mater Struct/Mater Const 55(4):1–17. https://doi.org/10.1617/s11527-021-01806-7
12. Marcos-Meson V, Michel A, Solgaard A, Fischer G, Edvardsen C, Skovhus TL (2017) Corrosion resistance of steel fibre reinforced concrete - a literature review. Cem Concr Res 103:1–20. https://doi.org/10.1016/j.cemconres.2017.05.016
13. Chen G, Hadi MNS, Gao D, Zhao L (2015) Experimental study on the properties of corroded steel fibres. Constr Build Mater 79:165–172. https://doi.org/10.1016/j.conbuildmat.2014.12.082
14. Söylev TA, Özturan T (2014) Durability, physical and mechanical properties of fiber-reinforced concretes at low-volume fraction. Constr Build Mater 73:67–75. https://doi.org/10.1016/j.conbuildmat.2014.09.058
15. Anandan S, Vallarasu Manoharan S, Sengottian T (2014) Corrosion effects on the strength properties of steel fibre reinforced concrete containing slag and corrosion inhibitor. Int J Corros 11:1–7. https://doi.org/10.1155/2014/595040
16. Qian CX, Stroeven P (2000) Development of hybrid polypropylene-steel fibre-reinforced concrete. Cem Concr Res 30(1):63–69. https://doi.org/10.1016/S0008-8846(99)00202-1
17. Yin S, Tuladhar R, Shi F, Combe M, Collister T, Sivakugan N (2015) Use of macro plastic fibres in concrete: a review. Constr Build Mater 93:180–188. https://doi.org/10.1016/j.conbuildmat.2015.05.105
18. Romanazzi V, Micelli F, Moro S, Aiello A, and Kandalaft AG (2022) Very high-performance fiber reinforced concrete (VHPFRC) testing and finite element analysis. *Recent Advances in Concrete Technology and Sustainability Issues - Conference Proceedings SP-355*, 2022
19. Meng C, Li W, Cai L, Shi X, Jiang C (2020) Experimental research on durability of high-performance synthetic fibers reinforced concrete: resistance to sulfate attack and freezing-thawing. Constr Build Mater 262:120055. https://doi.org/10.1016/j.conbuildmat.2020.120055
20. Ghanem SY, Bowling J, Sun Z (2021) Mechanical properties of hybrid synthetic fiber reinforced self- consolidating concrete. Compos Open Access 5:100154. https://doi.org/10.1016/j.jcomc.2021.100154
21. Banthia N, Gupta R (2006) Influence of polypropylene fiber geometry on plastic shrinkage cracking in concrete. Cem Concr Res 36(7):1263–1267. https://doi.org/10.1016/j.cemconres.2006.01.010
22. Won JP, Lim DH, Park CG (2006) Bond behaviour and flexural performance of structural synthetic fibre-reinforced concrete. Mag Concr Res 58(6):401–410. https://doi.org/10.1680/macr.2006.58.6.401
23. Oh BH, Kim JC, Choi YC (2007) Fracture behavior of concrete members reinforced with structural synthetic fibers. Eng Fract Mech 74(1–2):243–257. https://doi.org/10.1016/j.engfracmech.2006.01.032
24. Buratti N, Mazzotti C, Savoia M (2011) Post-cracking behaviour of steel and macro-synthetic fibre-reinforced concretes. Constr Build Mater 25(5):2713–2722. https://doi.org/10.1016/j.conbuildmat.2010.12.022
25. Pakravan HR, Ozbakkaloglu T (2019) Synthetic fibers for cementitious composites: a critical and in-depth review of recent advances. Constr Build Mater 207:491–518. https://doi.org/10.1016/j.conbuildmat.2019.02.078
26. Pakravan HR, Memariyan F (2017) Modification of low-surface energy fibers used as reinforcement in cementitious composites: a review. Polym-Plast Technol 56:227–239
27. Behfarnia K, Behravan A (2014) Application of high performance polypropylene fibers in concrete lining of water tunnels. Mater Des 55:274–279. https://doi.org/10.1016/j.matdes.2013.09.075
28. Aslani F, Nejadi S (2013) Self-compacting concrete incorporating steel and polypropylene fibers: Compressive and tensile strengths, moduli of elasticity and rupture, compressive stress–strain curve, and energy dissipated under compression. Compos B Eng 53:121–133. https://doi.org/10.1016/j.compositesb.2013.04.044
29. Gencel O, Ozel C, Brostow W, Martínez-Barrera G (2011) Mechanical properties of self-compacting concrete reinforced with polypropylene fibres. Mater Res Innovations 15(3):216–225. https://doi.org/10.1179/143307511X13018917925900

30. Sun Z, Xu Q (2009) Microscopic, physical and mechanical analysis of polypropylene fiber reinforced concrete. Mater Sci Eng, A 527(1–2):198–204. https://doi.org/10.1016/j.msea.2009.07.056
31. Sadrinejad I, Madandoust R, Ranjbar MM (2018) The mechanical and durability properties of concrete containing hybrid synthetic fibers. Constr Build Mater 178:72–82. https://doi.org/10.1016/j.conbuildmat.2018.05.145
32. Hubert M, Desmettre C, Charron JP (2015) Influence of fiber content and reinforcement ratio on the water permeability of reinforced concrete. Mater Struct Mater Const 48(9):2795–2807. https://doi.org/10.1617/s11527-014-0354-z
33. Ramezanianpour AA, Esmaeili M, Ghahari SA, Najafi MH (2013) Laboratory study on the effect of polypropylene fiber on durability, and physical and mechanical characteristic of concrete for application in sleepers. Constr Build Mater 44:411–418. https://doi.org/10.1016/j.conbuildmat.2013.02.076
34. Kakooei S, Akil HM, Jamshidi M, Rouhi J (2012) The effects of polypropylene fibers on the properties of reinforced concrete structures. Constr Build Mater 27(1):73–77. https://doi.org/10.1016/j.conbuildmat.2011.08.015
35. UNI EN 12390–3, Testing hardened concrete - Part 3: Compressive strength of test specimens 2001
36. UNI EN 12390–13, Testing hardened concrete - Part 13: Determination of secant modulus of elasticity in compression, 2013
37. UNI EN 14651, Test method for metallic fibered concrete - Measuring the flexural tensile strength. 2005
38. ASTM C1609/C 1609M - 07, "Standard test method for flexural performance of fiber-reinforced concrete (using beam with third-point loading)," 2009
39. UNI EN 12390–8, "Testing hardened concrete - Part 8: Depth of penetration of water under pressure," 2019
40. UNI EN 12350–8, "Testing fresh concrete - Part 8: Self-compacting concrete - Slump-flow test," 2010
41. Wang J, Dai Q, Si R, Guo S (2018) Investigation of properties and performances of polyvinyl alcohol (PVA) fiber-reinforced rubber concrete. Constr Build Mater 193:631–642. https://doi.org/10.1016/j.conbuildmat.2018.11.002
42. Hossain KMA, Lachemi M, Sammour M, Sonebi M (2012) Influence of polyvinyl alcohol, steel, and hybrid fibers on fresh and rheological properties of self-consolidating concrete. J Mater Civ Eng 24(9):1211–1220. https://doi.org/10.1061/(asce)mt.1943-5533.0000490
43. Noushini A, Hastings M, Castel A, Aslani F (2018) Mechanical and flexural performance of synthetic fibre reinforced geopolymer concrete. Constr Build Mater 186:454–475. https://doi.org/10.1016/j.conbuildmat.2018.07.110
44. Soroushian P, Plasencia J, Ravanbakhsh S (2003) Assessment of reinforcing effects of recycled plastic and paper in concrete. ACI Mater J 100(3):203–207
45. Mudadu A, Tiberti G, Plizzari GA, Morbi A (2019) Post-cracking behavior of polypropylene fiber reinforced concrete under bending and uniaxial tensile tests. Struct Concr 20(4):1411–1424. https://doi.org/10.1002/suco.201800224
46. EN 1990, "Eurocode 0 - Basis of structural design," 2002
47. CEB-FIP, *Fib Model Code for Concrete Structures*. 2010. https://doi.org/10.1007/s13398-014-0173-7.2
48. RILEM TC-50 FMC (Draft Recommendation), "Determination of the fracture energy of mortar and concrete by means of three-point bend tests on notched beams," 1985. https://doi.org/10.1007/BF00962380

Publisher's Note Springer Nature remains neutral with regard to jurisdictional claims in published maps and institutional affiliations.